Original Article

Further exploration of MRI techniques for liver T1rho quantification

Feng Zhao[1], Jing Yuan[1,2], Min Deng[1], Pu-Xuan Lu[3], Anil T. Ahuja[1], Yi-Xiang J. Wang[1]

[1]Department of Imaging and Interventional Radiology, The Chinese University of Hong Kong, Prince of Wales Hospital, Shatin, N.T., Hong Kong, China; [2]Shenzhen Research Institute, The Chinese University of Hong Kong, Shenzhen, Guangdong Province, China; [3]Department of Radiology, The Shenzhen Third People's Hospital, Shenzhen, Guangdong Province, China

Corresponding to: Dr. Yi-Xiang Wang. Department of Imaging and Interventional Radiology, The Chinese University of Hong Kong, Prince of Wales Hospital, Shatin, N.T., Hong Kong, China. Email: yixiang_wang@cuhk.edu.hk.

Abstract: With biliary duct ligation and CCl4 induced rat liver fibrosis models, recent studies showed that MR T1rho imaging is able to detect liver fibrosis, and the degree of fibrosis is correlated with the degree of elevation of the T1rho measurements, suggesting liver T1rho quantification may play an important role for liver fibrosis early detection and grading. It has also been reported it is feasible to obtain consistent liver T1rho measurement for human subjects at 3 Tesla (3 T), and preliminary clinical data suggest liver T1rho is increased in patients with cirrhosis. In these previous studies, T1rho imaging was used with the rotary-echo spin-lock pulse for T1rho preparation, and number of signal averaging (NSA) was 2. Due to the presence of inhomogeneous B0 field, artifacts may occur in the acquired T1rho-weighted images. The method described by Dixon *et al.* (Magn Reson Med 1996;36:90-4), which is a hard RF pulse with 135° flip angle and same RF phase as the spin-locking RF pulse is inserted right before and after the spin-locking RF pulse, has been proposed to reduce sensitivity to B0 field inhomogeneity in T1rho imaging. In this study, we compared the images scanned by rotary-echo spin-lock pulse method (sequence 1) and the pulse modified according to Dixon method (sequence 2). When the artifacts occurred in T1rho images, we repeated the same scan until satisfactory. We accepted images if artifact in liver was less than 10% of liver area by visual estimation. When NSA =2, the breath-holding duration for data acquisition of one slice scanning was 8 sec due to a delay time of 6,000 ms for magnetization restoration. If NSA =1, the duration was shortened to be 2 sec. In previous studies, manual region of interest (ROI) analysis of T1rho map was used. In this current study, histogram analysis was also applied to evaluate liver T1rho value on T1rho maps. MRI data acquisition was performed on a 3 T clinical scanner. There were 29 subjects with 61 examinations obtained. Liver T1rho values obtained by sequence 1 (NSA =2) and sequence 2 (NSA =2) showed similar values, i.e., 43.1±2.1 ms (range: 38.6-48.0 ms, n=40 scans) *vs.* 43.5±2.5 ms (range: 39.0-47.7 ms, n=12 scans, P=0.74) respectively. For the six volunteers scanned with both sequences in one session, the intraclass correlation coefficient (ICC) was 0.939. Overall, the success rate of obtaining satisfactory images per acquisition was slightly over 50% for both sequence 1 and sequence 2. Satisfactory images can usually be obtained by asking the volunteer subjects to better hold their breath. However, sequence 2 did not increase the scan success rate. For the nine subjects scanned by sequence 2 with both NSA =2 and NSA =1 during one session, the ICC was 0.274, demonstrated poor agreement. T1rho measurement by ROI method and histogram had an ICC of 0.901 (P>0.05), demonstrated very good agreement. We conclude that by including 135° flip angle before and after the spin-locking RF pulse, the rate of artifacts occurring did not decrease. On the other hand, sequence 1 and sequence 2 measured similar T1rho value in healthy liver. While reducing the breath—holding duration significantly, NSA =1 did not offer satisfactory signal-to-noise ratio. Histogram measurement can be adopted for future studies.

Keywords: Magnetic resonance imaging; liver; T1rho; quantification

Submitted Dec 13, 2013. Accepted for publication Dec 22, 2013.
doi: 10.3978/j.issn.2223-4292.2013.12.10
Scan to your mobile device or view this article at: http://www.amepc.org/qims/article/view/3109/3996

Introduction

Chronic liver disease is a major public health problem worldwide. Liver fibrosis, a common feature of almost all causes of chronic liver disease, involves the accumulation of collagen, proteoglycans, and other macromolecules within the extracellular matrix. Ultimately, progressive hepatic fibrosis leads to cirrhosis, in which fibrous bands carve the liver parenchyma into nodules of regenerating hepatocytes. The available diagnostic tests used in clinical practice, are not sensitive or specific enough to detect occult liver injury at early or intermediate stages (1). Liver biopsy is the standard of reference for the diagnosis and staging of liver fibrosis. However, it is an invasive procedure with possible complications. Histologic assessment of fibrosis is also an inherently subjective process, which is subject to sampling variability. A study that compared laparoscopic *vs.* histological diagnosis of cirrhosis found that 32% of cases were underdiagnosed with histological examination of a single liver biopsy specimen (2). Also, a number of studies have demonstrated excessive histological sampling error (25-40%), resulting in poor reproducibility regardless of underlying liver disease origin (3). In addition, interpretation variation by expert histopathologists may be as high as 20% (4). Liver biopsy also leads to hospitalization in 3% of cases, and has a fatality rate of 0.03% (5). These limitations make liver biopsy unsuitable for diagnosis and longitudinal monitoring in the general population. A reproducible and reliable non-invasive method is needed to evaluate disease progression in patients with chronic liver disease, to monitor treatment with conventional drugs and new drugs under development, and for epidemiological research (6).

T1rho relaxation time, or spin-lattice relaxation time, in the rotating frame, stands for the time constant for transverse magnetization decay in a very weak B1 field strength, produced by a continuous wave radiofrequency (RF) pulse, called spin-lock RF pulse, which applied along the transverse magnetization. As the spin-lock field strength is much weaker than the main magnetic field strength B0, T1rho relaxation time is considered similar to the T1 relaxation time at very low B0, and is sensitive to low frequency motional processes in physiology. With biliary duct ligation and carbon tetrachloride intoxication induced rat liver fibrosis models, recent studies showed that magnetic resonance (MR) T1rho imaging is able to detect liver fibrosis, and the degree of fibrosis is correlated with the degree of elevation of the T1rho measurements, suggesting that the liver T1rho quantification may play an important role for early detection and grading of liver fibrosis (7,8). Additionally, T1rho imaging has been applied for human liver and consistent liver T1rho measurement has been achieved for healthy volunteers at 3 Tesla (3 T) with multiple spin-lock times (SLTs) (9,10). Preliminary clinical data suggest liver T1rho is increased in patients with cirrhosis (11).

Using both theoretical simulation and practical validation (10,11), we reported it is possible to accelerate T1rho relaxation quantification in liver by using limited spin-lock time points (i.e., spin-lock time points =3). In our previous studies (7-12), T1rho imaging was used with the rotary-echo spin-lock pulse for T1rho preparation, and number of signal acquisition (NSA) was 2. Due to the presence of inhomogeneous B0 field, artifacts may occur in the acquired T1rho-weighted images. The method described by Dixon *et al.* (13), which is a hard RF pulse with 135° flip angle and same RF phase as the spin-locking RF pulse is inserted right before and after the spin-locking RF pulse, has been proposed to reduce sensitivity to B0 field inhomogeneity in T1rho imaging (13,14). In this current study, we compared the MR images acquired by rotary-echo spin-lock pulse method as we previously used, and images acquired with the pulse modified according to Dixon method. In our previous studies (9,10), the delay time for magnetization restoration was 6,000 ms. When NSA is 2, the total breath-holding duration for the data acquisition of one slice was 8 sec. If the NSA is 1, the duration can be reduced to be 2 sec, as the delay time for magnetization restoration for the second data acquisition is moved. Also in our previous studies, manual ROI analysis of T1rho map was used. In this current study, histogram analysis was applied to evaluate liver T1rho value on T1rho maps, and the results were compared with the measurements obtained with ROI based method.

Material and methods

The study was approved by the Institutional Ethics Committee, and all the subjects provided informed signed consent. All subjects were clinically healthy with no history of liver disease or alcoholism. MRI data acquisition was performed on a 3 T clinical scanner (Achieva, Philips Healthcare, Best, the Netherlands). An 8-channel cardiac coil was used as the signal receiver to cover the whole liver, and the built-in body coil was used as the signal transmitter. Subjects were examined in the supine position. Liver anatomical imaging covering the whole liver was carried out using a standard axial breath hold T2-weighted turbo

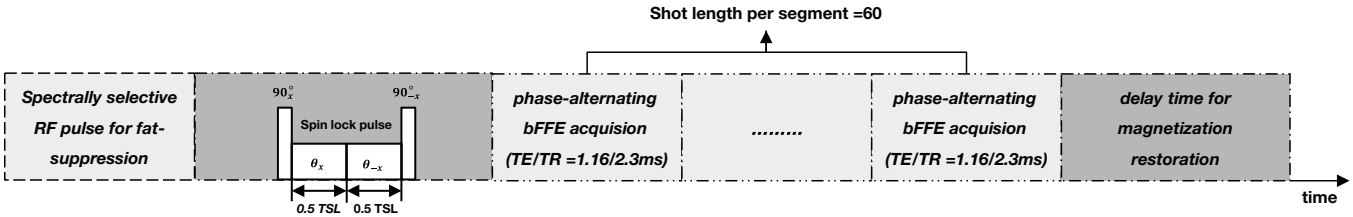

Figure 1 Diagram of the spin-lock balanced fast field echo (bFFE) imaging sequence for T1rho image (sequence 1). TSL = time of spin-lock pulse. The rotary-echo spin-lock pulse method was used for T1rho preparation.

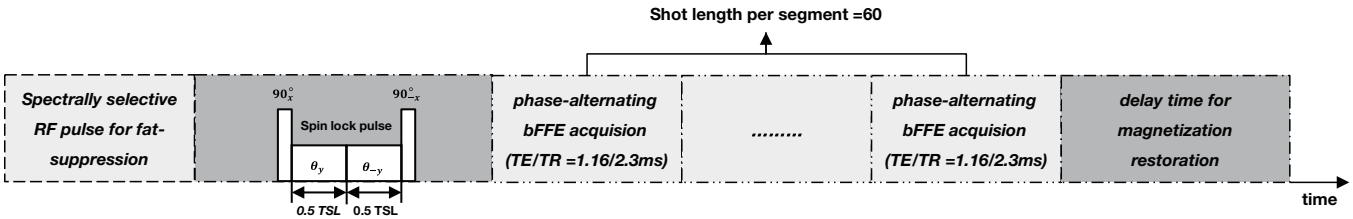

Figure 2 Diagram of the spin-lock balanced fast field echo (bFFE) imaging sequence for T1rho image (sequence 2). TSL = time of spin-lock pulse. The rotary-echo spin-lock pulse modified with Dixon method was used for T1rho preparation (13).

Table 1 Subject number of T1rho MR imaging with different MRI scan and data analysis protocols

Scanning protocol	Number of subject (n)		Number of scans performed (n)		Measurement method (n)	
	Volunteers reported*	New volunteers**	Volunteers reported*	New volunteer**	ROI	Histogram
Sequence 1, NSA =2	17	6	34	6	40	40
Sequence 2, NSA =2	0	12	0	12	12	12
Sequence 1 & 2, NSA =2	0	6	0	6		
Sequence 2, NSA =2 & =1	0	9	0	9		

*, Volunteers already reported in (9,10); **, additional volunteers recruited for this study.

spin echo pulse sequence with SPAIR (Spectral Adiabatic Inversion Recovery) fat suppression. The parameters included: TE =70 ms, TR =1,236 ms; Flip angle =90 degree; FOV =300×241×159 mm^3; voxel size =1×1.4×7 mm^3; Slice no. =20 slices; NSA =2. Using axial T2-weighted image as reference, representative axial slices were selected to cut through the liver for T1 rho imaging (9,10).

Volume shimming was employed to minimize the B0 inhomogeneity. For T1rho measurement, a rotary echo spin-lock pulse was implemented in a 2 dimensional single-shot fast field echo (FFE) sequence (sequence 1: *Figure 1*, sequence 2: *Figure 2*). Normal phase alternating FFE readout was used for the acquisition, and the phase encoding was in centric order. T1rho-weighted images were acquired during the transient status towards the steady-state, but with T1rho-weighted magnetization maintained. The flip angle was 40 degree, and the NSA was 2. A sensitivity-encoding factor of 1.5 was applied for parallel imaging to reduce the phase. Spin-lock frequency was set as 500 Hz and the spin-lock times of 1, 20, and 50 ms were used for T1rho mapping (10,11). TE and TR for FFE acquisition were 1.16 and 2.3 ms respectively. The voxel size was 1.50×1.50×7.00 mm^3. The subjects of T1rho MR imaging with different protocols were listed in the *Table 1*.

Seventeen healthy subjects with 34 scans scanned with method 1 and NSA =2 was reported in our previous studies (9,10). Additional 12 healthy subjects were added in this study (3 females and 9 males, age: 26-33 years; mean: 29.8 years), they all underwent scanning with method 2 and NSA =2, six subjects were examined additionally with method 1, and 9 subjects were also scanned with NSA =1 (*Table 1*).

When the artifacts occurred in T1rho images, we repeated the same scan until satisfactory images were

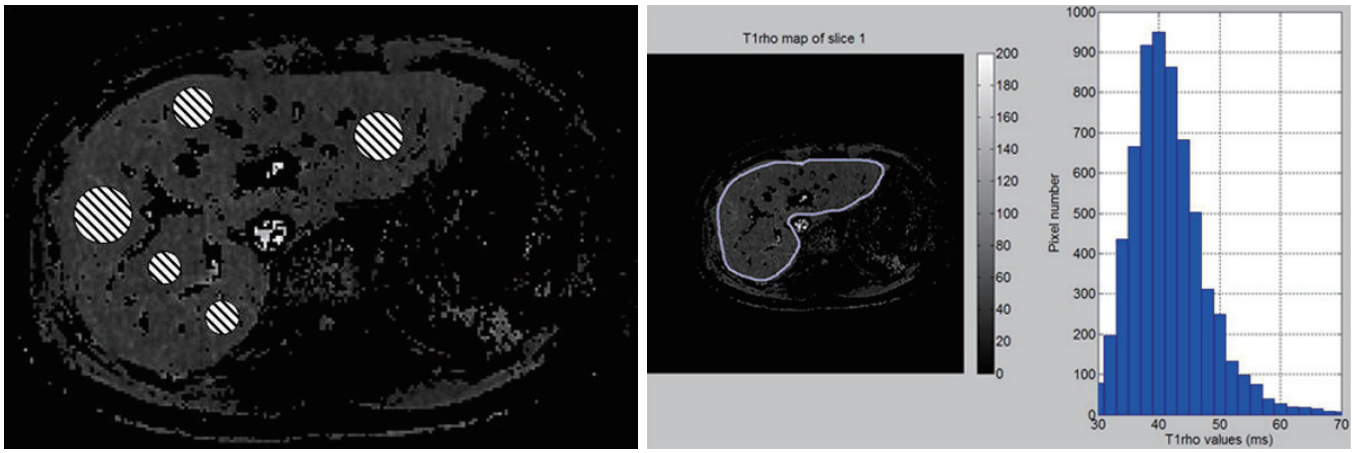

Figure 3 T1rho measurement methods [ROIs method (left), histogram method (right)] in one subject.

obtained. We accepted images if artifact in liver was less than 10% of liver area by visual estimation.

T1rho maps were constructed for T1rho weighted images. They were computed on a pixel-by-pixel basis, using a mono-exponential decay model, implemented in a home-made Matlab program (Mathworks, Natick, MA, USA):

$$M(SLT) = M0 \times \exp(-SLT/T1rho) \quad [1]$$

Where M0 and M (SLT) denote the equilibrium magnetization and T1rho-prepared magnetization with the spin lock time of SLT, respectively. This mono-exponential equation was linearized by taking the logarithm and T1rho maps were generated by fitting all the pixel intensity data as a function of SLT time, using linear regression. T1rho was calculated as –1/slope of the straight-line fit. Maps of the coefficient of determination R^2 were also generated for the evaluation of goodness of fit. Only T1rho values for the pixels satisfied with the goodness of fit to (R^2 >0.80) were included in the subsequent analysis. On T1rho map, this allows elimination of the unreliable poorly-fitted T1rho values due to the blood vessel contamination with fresh blood in-flow, as well as the respiration or pulsation induced artifacts.

For ROI based measurement, we quantified the T1rho values by setting five ROIs of 100-200 mm^2 on liver parenchyma region of each slice's T1rho maps (*Figure 3*) (9,10). The histogram was applied to the T1rho map to display the pixel values from the magnitude image. For histogram analysis, the liver parenchyma was included by contouring the liver border manually. Values were recorded except for those associated with the poor goodness of fit R^2 <0.80. Most blood vessel pixels and pixels notably contaminated by spin-lock artifacts could be well excluded by using this R^2 criterion. After that, the pixel-wise T1rho values were grouped in a histogram with equally spaced bins of 2 ms. The minimum and maximum of the histogram were assigned as 30 to 70 ms, respectively. In other word, the extreme pixel-wise T1rho values outside the range of 30-70 ms, which were thought to suffer from partial volume effects so compromise the true T1rho, were also excluded for histogram analysis. Each pixel was assigned to the bin that surrounds its associated T1rho value. The number of pixels corresponding to each bin was counted, and these counts were plotted as a function of the bin locations (*Figure 3*). The mean T1rho value for the highest bin was recorded and compared with the T1rho values measured by ROIs method. For example, in *Figure 3*, the T1rho values in five ROIs were 42.5, 41.5, 39.5, 41.1, and 38.9 ms, leading to a mean value of 40.7 ms. Meanwhile, in *Figure 3*, the highest bar in the histogram was the one within 39-41 ms, indicating the most frequent T1rho value range (~940 pixels, the height of the bar) in the whole liver parenchyma. The mean T1rho value for the pixels within this highest bar led to a value of 40.5 ms with the histogram method.

All statistical analyses were performed with software (SPSS, version 14.0; SPSS, Chicago, Ill). Mann-Whitney U test was used for nonpaired comparisons, and Wilcoxon signed rank test was used for paired comparisons. All statistical tests were two-sided. A P value less than 0.05 was considered to indicate a significant difference.

Results

Liver T1rho values obtained by sequence 1 with a NSA of 2

Table 2 Percentage of satisfactory images per acquisition using sequence 1 or sequence 2

Scanning protocol	Percentage of satisfactory images per acquisition (%)		
	SL01	SL20	SL50
Sequence 1	70.0	55.8	59.0
Sequence 2	60.5	51.1	56.1

SL01, time of spin-lock pulse =1 millisecond; SL20, time of spin-lock pulse =20 millisecond; SL50, time of spin-lock pulse =50 millisecond.

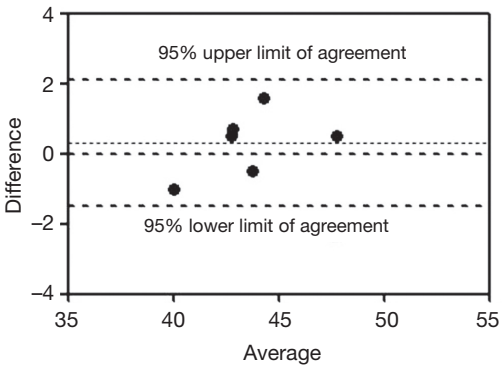

Figure 4 Bland and Altman plots for comparison of sequence 1 *vs.* sequence 2 (the Dixon method, n=6 subjects, x axis: T1 rho value in ms).

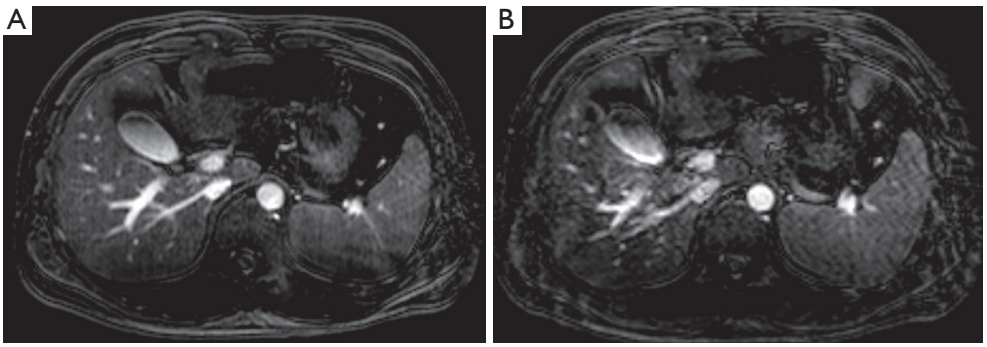

Figure 5 T1rho images from a patient acquired with sequence 2 with A has a NSA =2 and B has a NSA =1. The spin lock time was 50 ms.

and sequence 2 with a NSA of 2 showed similar values, i.e., 43.1±2.1 ms (range: 38.6-48.0 ms, n=40 scans) *vs.* 43.5±2.5 ms (range: 39.0-47.7 ms, n=12 scans) respectively. There was no statistical significance between them (P=0.74). For the 6 volunteers scanned with both sequences in one session, the ICC was 0.939 (by ROI measurement). The Bland and Altman analysis showed a mean difference of 0.3 (95% limits of agreement: –1.51, 2.11), therefore a very good agreement was achieved (*Figure 4*).

The percentage of images without obvious artifacts (less than 10% of liver area) for sequence 1 and sequence 2 in each slice was listed in *Table 2*. Overall, the success rate of obtaining satisfactory images per acquisition was slightly over 50%. Satisfactory images can usually be obtained by asking the volunteer subjects to better hold their breath. This study shows sequence 2 did not increase the scanning success rate (*Table 2*).

Images acquired with NSA =1 all had much slower signal-to-noise ratio than images acquired with NSA =2 (*Figure 5*). For the 9 subjects scanned by sequence 2 with both NSA =2 and NSA =1 during one session, the ICC was 0.274. The Bland and Altman analysis showed a mean difference of 5.01 (95% limits of agreement: –7.20, 17.22), indicating a poor agreement (*Figure 6*).

The T1rho values measured by ROI method and histogram method are shown in *Figure 7*. These two methods for T1rho measurement in all examinations (sequence 1 & 2, NSA =2, n=52 scans) had an ICC of 0.901. The Bland and Altman analysis showed a mean difference of 0.32 (*Figure 8*, 95% limits of agreement: –1.59, 2.24).

Discussion

In patients with pre-cirrhotic stages of the liver fibrosis as well as patients with early cirrhosis, the liver parenchyma usually has a normal appearance or may exhibit only subtle, nonspecific heterogeneity on conventional imaging techniques (15,16). Recently, a number of novel MR imaging techniques are being investigated to identify or grade liver fibrosis (17). T1rho MRI has the advantage

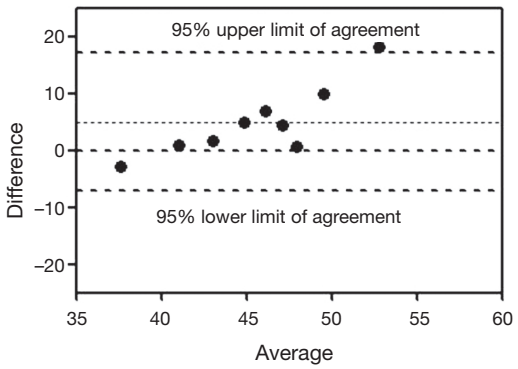

Figure 6 Bland and Altman plots for comparison of number of signal averaging (NSA) =2 and NSA =1 (n=9 subjects; x axis: T1 rho value in ms).

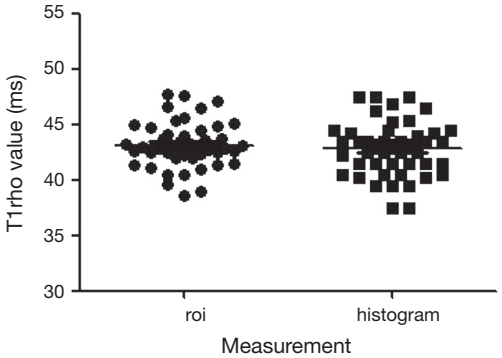

Figure 7 T1rho values measured by ROI method and histogram method in all subjects with number of signal averaging (NSA) =2 (n=52).

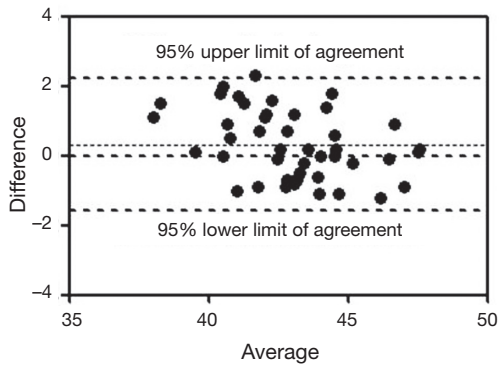

Figure 8 Bland and Altman plots for T1rho values measured by ROI method and histogram method (x axis: T1 rho value in ms).

that it does not involve additional intravenous injection of contrast agent or external driver (18,19). With further technical optimization, T1rho MRI may be a potential important biomarker for liver fibrosis early grading, evaluation of disease progression, and monitoring responses to drug treatment (7-10,12).

Our results suggested by including 135° flip angle before and after the spin-locking RF pulse, the rate of artifacts occurring did not decrease. A plausible explanation for this is the fact that the tissue of interest and the spin-lock imaging setting in this study were different from those in Dixon's paper. First, the composite spin-lock pulse in Dixon's method was originally proposed for heart at 1.5 T, whose intrinsic relaxation times (T1 and T2) are different from liver at 3 T in this study and hence influence magnetization evolution under spin locking. More importantly, the tolerance of the Dixon's composite spin-lock pulse to field inhomogeneity is much dependent on spin-lock frequency and spin-lock time. This is the major reason that the Dixon's composite spin-lock pulse was originally proposed with a fixed spin-lock frequency and spin-lock time optimized for myocardial suppression in T1rho-weighted imaging. As comparison, our study involved the use of different spin-lock times for T1rho mapping and a much stronger spin-lock frequency than that in the Dixon's study (500 Hz *vs.* ~125 Hz). As such, the effectiveness of Dixon's method for artifact reduction may be compromised with the variation of spin-lock times at substantially different spin-lock field strength. On the other hand, sequence 1 and sequence 2 measured similar T1rho value in healthy liver which indicates the liver T1rho value is not sequence specific.

Accurate and precise T1rho mapping is challenging under the scan time constraint because multiple SLTs are usually required, and a long delay time is also often necessary in the spin-lock pulse sequence for the longitudinal magnetization restoration. The reduction of the number of averaging is an apparent strategy to enhance T1rho imaging efficiency, if the accuracy and reliability of T1rho mapping could be maintained. If NSA =1 can be applied, the breath-hold duration can be reduced from 8 to 2 sec, it will be very advantageous for patients who experience difficulties in holding their breath. Also it is more likely that patients will hold the breath very well for the 2 sec duration than for 8 sec duration. Examinations with fewer NSAs are also helpful to reduce the total RF energy deposition into the patient bodies, and mitigating the safety concern. However, in our experiment it was shown that while reducing the breath-holding duration significantly, NSA =1 showed noisy images and the measured T1rho values had a very poor agreement compared with results from NSA =2.

ROIs measurement has an unavoidable component of

inter- and intra-observer variability. Reliable, reproducible data may only be obtained by experienced operators. Developing a more objective method will allow even an inexperienced operator to obtain reliable and potentially more reproducible data. The results that histogram measurement and manual ROI measurement provided similar liver T1rho value are reassuring. Our study suggests that histogram measurement can be used for future studies. Previously, we reported healthy liver T1ho measurement in 17 subjects, and additional 12 subjects are reported in this study. Pool all the results together (n=52 examinations), our data showed a mean liver T1rho value of 43.2±2.2 ms, with a range of 38.6-48.0 ms.

In conclusion, our study tried to improve the MRI T1rho measurement in liver in human subjects. The results suggested by including 135° flip angle before and after the spin-locking RF pulse (the Dixon method) the rate of artifacts occurring did not decrease. On the other hand, with or without including 135° flip angle before and after the spin-locking RF pulse showed similar T1rho value in healthy liver. While reducing the breath-holding duration significantly, T1rho measurement with NSA =1 showed unreliable results. The histogram measurement and manual ROI measurement provided similar liver T1rho value, therefore histogram measurement can be adopted for future studies.

Acknowledgements

This study is supported by RGC General Research Fund (475911), by a direct grant for research of The Chinese University of Hong Kong (2041607), by China NSFC grant 81201076, and partially by a grant from the Research Grants Council of the Hong Kong SAR (Project No.SEG_CUHK02).

The authors like to thank Dr. Xiaojuan Li at Department of Radiology, University of California at San Francisco, for helpful suggestions for this study.

Disclosure: The authors declare no conflict of interest.

References

1. Afdhal NH, Nunes D. Evaluation of liver fibrosis: a concise review. Am J Gastroenterol 2004;99:1160-74.
2. Poniachik J, Bernstein DE, Reddy KR, et al. The role of laparoscopy in the diagnosis of cirrhosis. Gastrointest Endosc 1996;43:568-71.
3. Ratziu V, Charlotte F, Heurtier A, et al. Sampling variability of liver biopsy in nonalcoholic fatty liver disease. Gastroenterology 2005;128:1898-906.
4. Bravo AA, Sheth SG, Chopra S. Liver biopsy. N Engl J Med 2001;344:495-500.
5. Janes CH, Lindor KD. Outcome of patients hospitalized for complications after outpatient liver biopsy. Ann Intern Med 1993;118:96-8.
6. Friedman SL, Bansal MB. Reversal of hepatic fibrosis -- fact or fantasy? Hepatology 2006;43:S82-8.
7. Wang YX, Yuan J, Chu ES, et al. T1rho MR imaging is sensitive to evaluate liver fibrosis: an experimental study in a rat biliary duct ligation model. Radiology 2011;259:712-9.
8. Zhao F, Wang YX, Yuan J, et al. MR T1ρ as an imaging biomarker for monitoring liver injury progression and regression: an experimental study in rats with carbon tetrachloride intoxication. Eur Radiol 2012;22:1709-16.
9. Deng M, Zhao F, Yuan J, et al. Liver T1ρ MRI measurement in healthy human subjects at 3 T: a preliminary study with a two-dimensional fast-field echo sequence. Br J Radiol 2012;85:e590-5.
10. Zhao F, Deng M, Yuan J, et al. Experimental evaluation of accelerated T1rho relaxation quantification in human liver using limited spin-lock times. Korean J Radiol 2012;13:736-42.
11. Yuan J, Zhao F, Griffith JF, et al. Optimized efficient liver T(1ρ) mapping using limited spin lock times. Phys Med Biol 2012;57:1631-40.
12. Wang YX, Zhao F, Wong VW, et al. Liver MR T1rho measurement in liver cirrhosis patients: a preliminary study with a 2D fast field echo sequence at 3T. Paper presented in the 20th Annual Meeting & Exhibition of ISMRM, 2012:1289.
13. Dixon WT, Oshinski JN, Trudeau JD, et al. Myocardial suppression in vivo by spin locking with composite pulses. Magn Reson Med 1996;36:90-4.
14. Chen W, Takahashi A, Han E. Quantitative T(1) (ρ) imaging using phase cycling for B0 and B1 field inhomogeneity compensation. Magn Reson Imaging 2011;29:608-19.
15. Faria SC, Ganesan K, Mwangi I, et al. MR imaging of liver fibrosis: current state of the art. Radiographics 2009;29:1615-35.
16. Ito K, Mitchell DG. Imaging diagnosis of cirrhosis and chronic hepatitis. Intervirology 2004;47:134-43.
17. Talwalkar JA, Yin M, Fidler JL, et al. Magnetic resonance imaging of hepatic fibrosis: emerging clinical applications. Hepatology 2008;47:332-42.

18. Aguirre DA, Behling CA, Alpert E, et al. Liver fibrosis: noninvasive diagnosis with double contrast material-enhanced MR imaging. Radiology 2006;239:425-37.
19. Venkatesh SK, Wang G, Lim SG, et al. Magnetic resonance elastography for the detection and staging of liver fibrosis in chronic hepatitis B. Eur Radiol 2014;24:70-8.

Cite this article as: Zhao F, Yuan J, Deng M, Lu PX, Ahuja AT, Wang YX. Further exploration of MRI techniques for liver T1rho quantification. Quant Imaging Med Surg 2013;3(6):308-315. doi: 10.3978/j.issn.2223-4292.2013.12.10

